

# Stability of the trapped nonconservative Gross-Pitaevskii equation with attractive two-body interaction

Victo S. Filho,<sup>1</sup> T. Frederico,<sup>2</sup> Arnaldo Gammal,<sup>1,3</sup> and Lauro Tomio<sup>1</sup>

<sup>1</sup>*Instituto de Física Teórica, Universidade Estadual Paulista, 01405-900, São Paulo, Brazil*

<sup>2</sup>*Departamento de Física, Instituto Tecnológico da Aeronáutica, CTA, 12228-900, São José dos Campos, Brazil*

<sup>3</sup>*Instituto de Física, Universidade de São Paulo, 05315-970, São Paulo, Brazil*

(Received 13 April 2002; published 27 September 2002)

The dynamics of a nonconservative Gross-Pitaevskii equation for trapped atomic systems with attractive two-body interaction is numerically investigated, considering wide variations of the nonconservative parameters, related to atomic feeding and dissipation. We study the possible limitations of the mean-field description for an atomic condensate with attractive two-body interaction, by defining the parameter regions, where stable or unstable formation can be found. The present study is useful and timely considering the possibility of large variations of attractive two-body scattering lengths, which may be feasible in recent experiments.

DOI: 10.1103/PhysRevE.66.036225

PACS number(s): 05.45.Mt, 05.45.Pq, 03.75.Fi, 32.80.Pj

## I. INTRODUCTION

The stability of the condensed state is governed by the nature of the effective atom-atom interaction, the two-body pseudopotential is repulsive for a positive  $s$ -wave atom-atom scattering length and it is attractive for a negative scattering length [1]. The ultracold trapped atoms with repulsive two-body interaction undergoes a phase transition to a stable condensed state, in several cases found experimentally, as for  $^{87}\text{Rb}$  [2],  $^{23}\text{Na}$  [3], and  $^1\text{H}$  [4]. However, a condensed state of atoms with negative  $s$ -wave atom-atom scattering length [as in case of  $^7\text{Li}$  [5]] would be unstable, unless the number of atoms  $N$  is small enough such that the stabilizing force provided by the zero-point motion and the harmonic trap overcomes the attractive interaction, as found on theoretical grounds [6,7]. Particularly, in the case of  $^7\text{Li}$  gas [5], for which the  $s$ -wave scattering length is  $a = -14.5 \pm 0.4 \text{ \AA}$ , it was experimentally observed that the number of allowed atoms in the Bose condensed state was limited to a maximum value between 650 and 1300, a result consistent with the mean-field prediction [6], where the term proportional to the two-body scattering length (negative) dominates the nonlinear part of the interaction.

More recently, the maximum critical number of atoms for Bose-Einstein condensates with two-body attractive interactions have been deeply investigated by the JILA group, considering experiments with  $^{85}\text{Rb}$  [8]. They have considered a wide tuning of the scattering length  $a$  from negative to positive, by means of Feshbach resonance [9,10], and observed that the system collapses for a number of atoms smaller than the theoretically predicted number. Their experimental results, when compared with theoretical predictions for spherical traps, show a deviation of up to 20% in the critical number. More precisely, it was shown in Ref. [11] that part of this discrepancy is due to the nonspherical symmetry that was considered in Ref. [8]. Such a deviation can also be an indication of higher order nonlinear effects that one should take into account in the mean-field description. In Ref. [12], it was considered the possibility of a real and positive quintic term, due to three-body effects, in the Gross-Pitaevskii for-

malism. A negative quintic term would favor the collapse of the system for a smaller critical number of atoms, as verified in the JILA's experiments. However, the real significance of a quintic term in the formalism is still an open question.

Our main motivation in the present work is to analyze the dynamics represented by an extension of the mean-field or Gross-Pitaevskii approximation, with nonconservative imaginary terms that are added to the real part of the effective interaction, the two-body nonlinear term with a spherically symmetric harmonic trap. For the imaginary part, the interaction is a combination of a linear term, related to atomic feeding, and a quintic term, due to three-body recombination, that is responsible for the atomic dissipation. This is an approximation that is commonly used to study the properties of Bose-Einstein condensed systems. We consider a wide variation of the nonconservative parameters, in particular motivated by the actual realistic scenario, that already exists, of altering experimentally the two-body scattering length [10]. As it will be clear in the following, this possibility will lead effectively to a modification of the dissipation parameter. By changing the absolute value of the scattering length, from zero to very large absolute values, one can change in an essential way the behavior of the mean-field description. As it will be shown from the present numerical approach, the results for the dynamical observables of the system can be very stable (solitonic type) or very unstable (chaotic type); the characteristic of the results will depend essentially on the ratio between the nonconservative parameters related to the atomic feeding and dissipation.

In the following section, we review the formalism. The main results are presented in Sec. III, followed by our conclusions in Sec. IV.

## II. MEAN-FIELD APPROXIMATION

The mean-field approximation has shown to be appropriate to describe atomic Bose-Einstein condensation of a dilute gas of atoms confined by a magnetic trap [13]. In the case of positive scattering length, we have a very good agreement with experimental data, as the thermal cloud is practically absent (removed by cooling evaporation) and almost all the

particles are in the condensed state. In this case, the mean-field approximation results in a nonlinear Schrödinger equation known as Gross-Pitaevskii equation (GPE). If we have  $N$  particles trapped in a spherical harmonic potential, this equation is given by

$$i\hbar \frac{\partial \Psi}{\partial t} = \left( -\frac{\hbar^2}{2m} \vec{\nabla}^2 + \frac{1}{2} m \omega^2 r^2 + \frac{4\pi\hbar^2 a}{m} |\Psi|^2 \right) \Psi, \quad (1)$$

where  $\Psi \equiv \Psi(\vec{r}, t)$ , the wave function of the condensate, is normalized to the number  $N$ ,  $m$  is the mass of a single atom,  $\omega$  is the angular frequency of the trap, and  $a$  is the two-body scattering length.

In this work, we have concentrated our study on the interesting dynamics that occurs when the scattering length is negative ( $a = -|a|$ ). In this case, it is well known that the system is unstable without the harmonic trap, and the trapped system has a critical limit  $N_c$  in the number of condensed atoms. The mean-field approximation has also shown to be reliable in determining the critical number of particles and even collapse cycles in the condensate [5,14,15]. Actually, systems with attractive two-body interaction are being intensively investigated experimentally [8], by using the so-called Feshbach resonance [9,10]. The scattering length can be tuned over a large range by adjusting an external magnetic field [for more details, see Ref. [16]]. Here, we are interested in the dynamics of a realistic system, where we add two nonconservative terms: one (linear) related to the atomic feeding from the nonequilibrium thermal cloud; and another, dissipative due to three-body recombination processes (quintic). It is true that other dissipative terms can also be relevant for an arbitrary trapped atomic system, as a cubic one, that can be related with dipolar relaxation or with an imaginary part of the two-body scattering length. However, in order to simplify the study and better analyze the results, we restrict our considerations to the case that we have just one parameter related with the feeding and another related with dissipation. We have considered only the three-body recombination parameter for dissipation also motivated by the observation that, for higher densities, this term dominates the two-body loss [17]. So, for the generalization of Eq. (1), we add the imaginary terms in the interaction, such that

$$i\hbar \frac{\partial \Psi}{\partial t} = -\frac{\hbar^2}{2m} \vec{\nabla}^2 \Psi + \frac{1}{2} m \omega^2 r^2 \Psi + \frac{4\pi\hbar^2 a}{m} |\Psi|^2 \Psi + iG_\gamma \Psi - iG_\xi |\Psi|^4 \Psi, \quad (2)$$

where  $G_\xi$  is the dissipation parameter, due to three-body collisions, and  $G_\gamma$  is a parameter related to the feeding of the condensate from the thermal cloud. The Eq. (2) was first suggested in Ref. [14] to simulate the condensation of  $^7\text{Li}$ .

In order to recognize easily the physical scales in Eqs. (1) and (2), it is convenient to work with dimensionless units. By making the transformations

$$\vec{r} \equiv \sqrt{\frac{\hbar}{2m\omega}} \vec{x}, \quad t \equiv \frac{\tau}{\omega}, \quad (3)$$

$$G_\gamma \equiv \frac{\gamma}{2} \hbar \omega, \quad G_\xi \equiv 2\xi \left( \frac{4\pi|a|\hbar}{m\omega} \right)^2 \hbar \omega, \quad (4)$$

and

$$\Phi \equiv \Phi(x, \tau) \equiv \sqrt{8\pi|a|} |\vec{r}| \Psi(\vec{r}, t), \quad (5)$$

we obtain the radial dimensionless  $s$ -wave equation:

$$i \frac{\partial \Phi}{\partial \tau} = \left[ -\frac{d^2}{dx^2} + \frac{x^2}{4} - \frac{|\Phi|^2}{x^2} - 2i\xi \frac{|\Phi|^4}{x^4} + i\frac{\gamma}{2} \right] \Phi. \quad (6)$$

As  $\Psi(\vec{r}, t)$  is normalized to the number of atoms  $N(t)$  in Eq. (2), the corresponding time-dependent normalization of  $\Phi(x, \tau)$  is given by the reduced number  $n(\tau)$ :

$$\int_0^\infty dx |\Phi(x, \tau)|^2 = n(\tau) \equiv 2N(t)|a| \sqrt{\frac{2m\omega}{\hbar}}. \quad (7)$$

The nonconservative GPE (6) is valid in the mean-field approximation of the quantum many-body problem of a dilute gas, when the average interparticle distances are much larger than the absolute value of the scattering length; and also when the wavelengths are much larger than the average interparticle distance. The nonconservative terms are important when the condensate oscillates, fed by the thermal cloud, while losing atoms due to three-body inelastic collisions, which happen mainly in the high density regions.

In order to verify the stability and the time evolution of the condensate, as observed in Refs. [18], two possible relevant observables are the number of particles normalized by the critical number of atoms of the static case [ $N(t)/N_c$ ] and the mean square radius,

$$\begin{aligned} \langle r^2(t) \rangle &= \left( \frac{\hbar}{2m\omega} \right) \frac{1}{n(\tau)} \int_0^\infty dx x^2 |\Phi(x, \tau)|^2 \equiv \left( \frac{\hbar}{2m\omega} \right) \langle x^2(\tau) \rangle \\ &\equiv \left( \frac{\hbar}{2m\omega} \right) X^2, \end{aligned} \quad (8)$$

where  $X \equiv \sqrt{\langle x^2(\tau) \rangle}$  is the dimensionless root mean-square radius. In our analysis of stability, we calculate the time evolution of these quantities. We explore several combinations of the dimensionless nonconservative parameters  $\xi$  and  $\gamma$ . We first consider the case in which the atomic feeding is absent or when its parameter is smaller than the atomic dissipation parameter. Next, we explore variations of both parameters of about five orders of magnitude, from  $10^{-5}$  to  $10^{-1}$ . This wide spectrum includes the parameters considered by Kagan *et al.* [14], as well as other combinations that can be considered more realistic due to recent experimental results [19].

Actually, the relevance of a wider relative variation of the nonconservative parameters  $\gamma$  and  $\xi$ , presented in Eq. (6), can be better appreciated in face of the experimental possibilities that exist to alter the two-body scattering length [10]. As one should note from Eq. (4), any variation of the scattering length will also affect the effective dissipation parameter  $\xi$  and, consequently, its relation with the feeding param-

eter  $\gamma$ . This implies that, by changing the value of the scattering length, from positive to negative, and from zero to very large absolute values, one can change in an essential way the behavior of the mean-field description. In the present work, we are concerned with negative two-body scattering length, where the collapsing behavior of the Eq. (6) shows a very interesting dynamical structure. Even considering the possible limitations on the validity of the mean-field approach after the first collapse (in cases of parametrization where it can occur), it is worthwhile to verify experimentally the behavior of a system in such a situation, by varying  $|a|$ . At least, one can verify how far the theoretical description can be qualitatively acceptable.

As already verified for systems with attractive interaction, as the  $^7\text{Li}$ , it has been possible, via the mean-field approach, to describe properties such as the critical number of atoms in the condensate and growth and collapse cycles [5,14,15]; besides, in the long time evolution, for certain sets of parameters, the calculations have also shown the presence of strong instabilities of the condensate, with signals of spatiotemporal chaotic behavior.

In order to characterize a chaotic behavior, it is necessary to show that the largest Lyapunov exponent related with the solutions of the equation is positive. We follow the criterion used by Deissler and Kaneko [20] to characterize spatiotemporal chaos. This criterion prescribes that the largest Lyapunov exponent for the system, in an arbitrary time interval, is obtained by plotting the logarithm of a function  $\zeta$ , which is defined by

$$\zeta(\tau) \equiv \left( \int_0^\tau |\delta\Phi(x, \tau)|^2 dx \right)^{1/2}. \quad (9)$$

$\delta\Phi(x, \tau)$  will give us the separation between two nearby trajectories; it is obtained in the following form, we numerically evolve in time an initial  $\Phi_0(x)$ , obtaining  $\Phi(x, \tau)$ . Independently, we evolve  $\Phi_0(x) + \epsilon(x)$ , and get  $\Phi'(x, \tau)$ , where  $\epsilon(x)$  is a very small random perturbation.  $\delta\Phi(x, \tau)$  is given by  $\Phi'(x, \tau) - \Phi(x, \tau)$ . The chaotic behavior is characterized by a positive slope of  $\ln \zeta(\tau)$ , which gives the largest Lyapunov exponent [20].

### III. NUMERICAL RESULTS

In the following, we present the most significant results that characterize the time evolution of the normalized number of particles  $[N(t)/N_c]$ , the dimensionless mean-square radius  $\langle x^2 \rangle$ , and, in order to characterize the stability of the system, the function related to the largest Lyapunov exponent. Further, we present a representative case of the phase space for the root mean-square radius. We have studied a wide region of parameters  $\gamma$  and  $\xi$ , covering about five orders of magnitude, from  $10^{-5}$  to  $10^{-1}$ , including the case with no feeding ( $\gamma=0$ ).

In order to have a clear and useful map of the regions where one should expect stable results, as well as regions with instabilities or chaos, we summarize the present numerical results in a diagrammatic picture that relates these two nonconservative parameters. In general, it is expected that

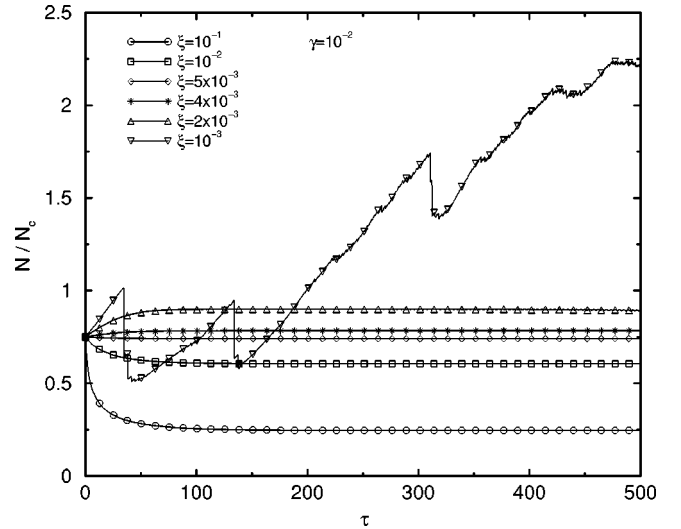


FIG. 1. Time evolution of the number of condensed atoms  $N$ , relative to the critical number  $N_c$ , for a set of values of the dissipative parameter  $\xi$  (as shown inside the frame), with the feeding parameter  $\gamma = 10^{-2}$ . All the quantities are in dimensionless units, as given in Eqs. (3) and (4).

the system is more stable when the parameter related to the feeding of atoms  $\gamma$  from the thermal cloud is significantly smaller than the parameter related to the dissipation  $\xi$ . However, it is interesting to find out the region of parameters where this transition (from stable to unstable results) occurs. Analysis of experimental results can provide a test to the present mean-field description in case of negative two-body interaction. As previously observed, we are considering dimensionless observables and parameters. For any realistic comparison with experimental parameters, one should convert  $\gamma$  and  $\xi$  to the parameters  $G_\gamma$  and  $G_\xi$ , as given in Eq. (4).

The numerical solutions of Eq. (6) were obtained by applying the semiimplicit Crank-Nicolson algorithm for nonlinear problems, as implemented in Ref. [18]. This method is stable and, therefore, very convenient and reliable to treat time-dependent nonlinear partial differential equations. The initial condition for the number of atoms  $N$  in the condensate was such that  $N(0)/N_c = n(0)/n_c = 0.75$ . The evolution of the observables have been extended upto  $\tau = \omega t = 500$ .

In general, as expected, the smaller is the dissipation parameter, the longer is the life of the condensate. The mean square radius presents an oscillatory behavior while one increases  $\xi$ . One observes that, in the regime of small feeding ( $\gamma \leq 10^{-4}$ ), the extended Lyapunov presents no positive slope. For larger values of  $\gamma$ , from  $\sim 10^{-3}$  and  $10^{-2}$ , we have studied a few cases where the interplay between the nonconservative behaviors are significant.

In Fig. 1, we show the dynamical behavior of the number of atoms for  $\gamma = 10^{-2}$  and several values of  $\xi$ ; and, in the Fig. 2, the corresponding time evolution of  $\langle x(\tau)^2 \rangle$ . We realize an interesting behavior, that occurs when the dissipation is larger than the feeding process: there are solutions of stability or dynamical equilibrium between both nonconservative processes. This phenomenon was already discussed in

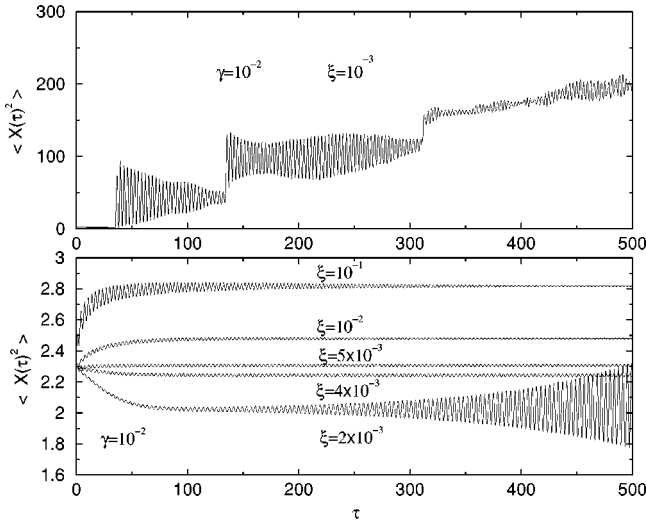


FIG. 2. Time evolution of the dimensionless mean-square radius  $\langle x(\tau)^2 \rangle$  for the feeding parameter  $\gamma = 10^{-2}$ . The results are given for a set of values of the dissipative parameter  $\xi$ , in the lower frame (shown inside). A specific case, for  $\xi = 10^{-3}$  (much smaller than  $\gamma$ ), is isolated in the upper frame, where one can observe the behavior of  $\langle x(\tau)^2 \rangle$  after the collapse. All the quantities are in dimensionless units, as given in Eqs. (3) and (4).

Ref. [21], for a few values of the dissipation and feeding parameters, using the time-dependent variational approach and also the Crank-Nicolson method. In the present work, we observe a wide region of parameters where it is possible the formation of autosolitons [21]. However, when the feeding process is much larger than the dissipation, of about one or more orders of magnitude, we can also observe chaotic behaviors. See, for example, the case with  $\xi = 10^{-3}$ .

The time evolution of the number of particles, represented in Fig. 1, shows a collapse for  $\tau \approx 30$ , followed by several other collapses, with the number of particles going above the critical limit  $N_c$ . So, after a sequence of collapses, the critical limit for the number of particles is no more followed, as already shown in Ref. [18].

The corresponding time evolution of  $\langle x(\tau)^2 \rangle$  is shown in the upper frame of Fig. 2. We observe that, following each collapse, after the shrinking of the system, the radius is multiplied by a large factor, with indication of being populated by radial excited states. In the lower frame of Fig. 2, we can observe the corresponding transition from the stable region (where the system finds the equilibrium at a fixed value of the radius, corresponding to autosoliton formation) to the unstable region. As shown, the instability starts to occur when  $\xi = 2 \times 10^{-3}$ , and it can be developed to a spatiotemporal chaos. The chaotic behavior can be verified through the Deissler-Kaneko criterion [20].

In Fig. 3 we illustrate the application of the Deissler-Kaneko criterion to the system given by Eq. (6), for a fixed value of the feeding parameter  $\gamma = 0.01$ , and a set of values of the dissipation parameter  $\xi$ . The time evolution of the function  $\ln(\zeta)$  was plotted, where  $\zeta$  is given by Eq. (9), following the prescription given in Ref. [20] to obtain the largest Lyapunov exponents for the system. Within this prescription, the system becomes chaotic when  $\ln(\zeta)$  has a positive

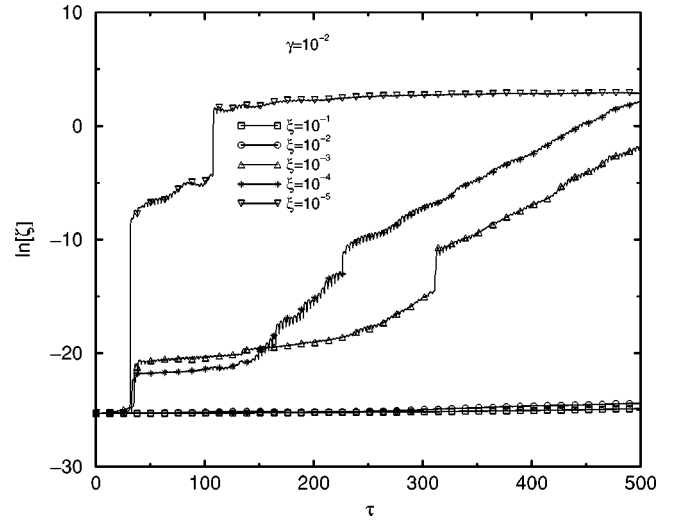


FIG. 3. Time evolution of  $\ln(\zeta)$ , related to the separation between two nearby trajectories [See Eq. (9)], for  $\gamma = 10^{-2}$  and a set of values of  $\xi$  indicated inside the figure. All the quantities are in dimensionless units, as given in Eqs. (3) and (4).

slope. As shown in Fig. 3, this clearly occurs, for example, when  $\xi = 10^{-4}$ . In case of  $\xi = 10^{-5}$  we note a much faster increasing in  $\ln(\zeta)$ , with an observed saturation that happens due to the fact that such function has reached the maximum separation between the trajectories. The saturation properties is also verified when studying chaotic behaviors in ordinary differential equations [22]. The plot of  $\ln(\zeta)$  corresponds to the same value of  $\gamma$  ( $= 10^{-2}$ ) used in Figs. 1 and 2. As shown, a clear characterization of chaotic behaviors starts to occur only for values of the dissipation parameter  $\xi$  much smaller than  $\gamma$ . In the cases presented in Fig. 3, for  $\xi \leq 10^{-3}$ .

In Fig. 4, we present another significant illustration of

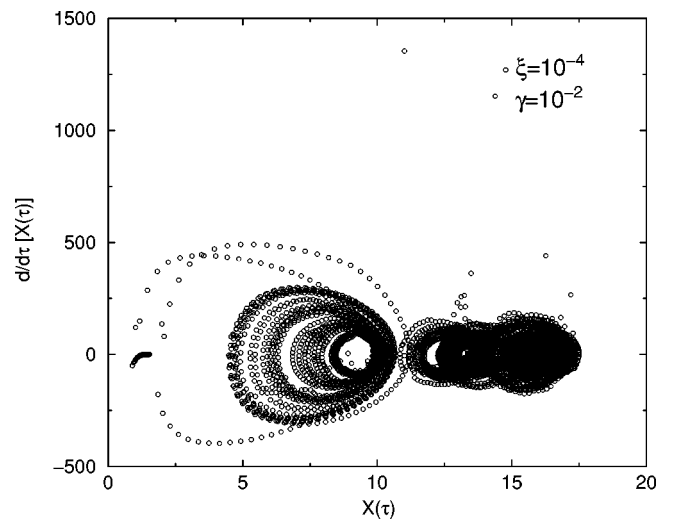


FIG. 4. Phase space for the root-mean-square radius, in dimensionless units [ $dX(\tau)/d\tau$  versus  $X(\tau)$ ], considering a collapsing case that leads to chaos. The dimensionless nonconservative parameters are  $\xi = 10^{-4}$  and  $\gamma = 10^{-2}$ , and the time evolution was taken up to  $t = \tau/\omega = 500/\omega$ .

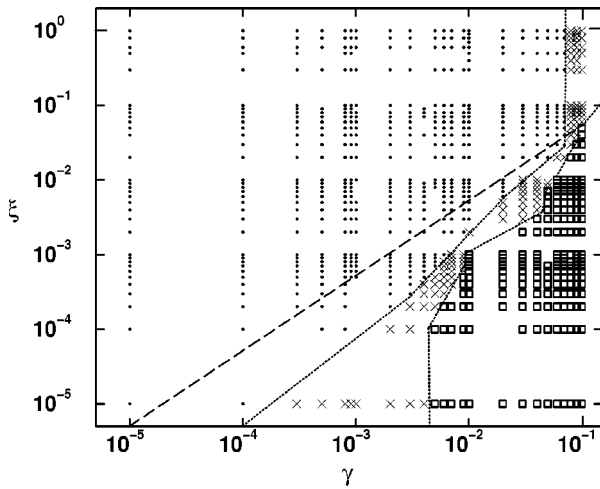


FIG. 5. Diagram for stability, according to the criterion of Ref. [20] given by Eq. (9), with results for the Eq. (6), considering the dimensionless nonconservative parameters  $\gamma$  and  $\xi$ . Between the unstable results, represented with  $\times$  and squares, the chaotic ones are identified with squares. The stable results are represented by bullets. Two dotted guidelines are splitting the regions. The dashed line splits the graph into two regions according to a variational approach [see Ref. [22]]; in the upper part the results are stable; in the lower, unstable.

chaotic behavior, through the phase-space behavior of the mean-square-radius, considering one case that was characterized as chaotic by using the Deissler-Kaneko criterion. We have plotted in this figure the root mean-square-radius phase space for the case with  $\gamma=0.01$  and  $\xi=10^{-4}$ . The irregular behavior of the trajectories, observed in Fig. 4, with the classical strange attractors being observed, clearly resembles chaos. This behavior is similar to the chaotic behavior observed in ordinary cases [22].

As a general remark that one can make from the presented results, we should note that, in order to observe unstable chaotic behaviors, the dissipation must be much smaller than the feeding parameter.

In a diagrammatic picture, given in Fig. 5, we resume our results. We show the relation between the two nonconservative parameters,  $\xi$  and  $\gamma$ , in order to characterize the parametric regions, where one should expect stability or instability in the solutions for the Eq. (6). The stable results of the Eq. (6) are represented by bullets; the nonstable results that clearly present positive slope for  $\ln \zeta(\tau)$  (chaotic behavior) are represented by empty squares; with  $\times$ , we show other intermediate nonstable results, in which the characterization of chaotic behavior was not so clear, through the Deissler-Kaneko criterion. In this figure, in order to observe the ap-

proximate consistency of the numerical results, we also include the variational analysis presented in Fig. 1 of Ref. [21], represented by the dashed line. It is separating the stable region (upper part) from the unstable one (lower part).

We should note that, in Sec. V of Ref. [23], it was also considered the dynamics of growth and collapse, with non-conservative terms related to feeding  $\gamma_0$  and dissipation  $\gamma_1$  and  $\gamma_2$  in a specific example. For the dissipation they have also considered a term related to dipolar relaxation, given by  $\gamma_2$ . Here, in our systematic study of the regions of instability, we took into account the previous experimental [8] observations that the dominant process for the dissipation is the three-body recombination. By comparing the parameters of Ref. [23] with the parameters that we have used, and observing that our parameter  $\xi$  should be related to both dissipation parameters used in Ref. [23] ( $\gamma=\gamma_0=2.6\times 10^{-3}$ ,  $\xi\sim 10^{-5}$ ) one can verify from the results given in Fig. 5 that the model of Ref. [23] is inside the intermediate region, where the system is unstable, without a clear signature of chaos.

#### IV. CONCLUSIONS

In summary, we have studied the dynamics associated with the extended nonconservative Gross-Pitaevskii equation for a wide region of the dimensionless nonconservative parameters,  $\xi$  and  $\gamma$ , that, respectively, are related to atomic dissipation and feeding in a trapped atomic condensed system. We consider systems with attractive two-body interaction in a spherically symmetric harmonic trap. In Fig. 5, we resume our results, by mapping the space of  $\gamma$  versus  $\xi$ , showing the regions of equilibrium and the regions of instability, as well as the regions where we are able to characterize chaotic behaviors, using a criterion given in Ref. [20]. It was also confirmed that chaotic behaviors occur mainly when  $\gamma$  is big enough and  $\gamma/\xi$  is large (at least, when  $\gamma$  is one or two orders of magnitude larger than  $\xi$ ). A wide variation of the nonconservative parameters was analyzed, in particular motivated by the actual realistic scenario, that already exists, of altering experimentally the two-body scattering length [10]. By changing the absolute value of the scattering length, one can change in an essential way the behavior of the mean-field description.

#### ACKNOWLEDGMENTS

We thank Fundação de Amparo à Pesquisa do Estado de São Paulo (FAPESP) for partial support. L.T. and T.F. also thank Conselho Nacional de Desenvolvimento Científico e Tecnológico (CNPq) for partial support.

- [1] K. Huang, *Statistical Mechanics*, 2nd ed. (Wiley, New York, 1987).
- [2] M.H. Anderson, E.J. Ensher, M.R. Matthews, C.E. Wieman, and E.A. Cornell, *Science* **269**, 198 (1995).
- [3] K.B. Davis, M.-O. Mewes, M.R. Andrews, N.J. van Druten,

- D.S. Durfee, D.M. Kurn, and W. Ketterle, *Phys. Rev. Lett.* **75**, 3969 (1995); M. R. Andrews, M.-O. Mewes, N. J. van Druten, D.S. Durfee, D.M. Kurn, and W. Ketterle, *Science* **273**, 84 (1996); M.-O. Mewes, M.R. Andrews, N.J. van Druten, D.M. Kurn, D.S. Durfee, and W. Ketterle, *Phys. Rev. Lett.* **77**, 416

- (1996).
- [4] D.G. Fried, T.C. Killian, L. Willmann, D. Landhuis, S.C. Moss, D. Kleppner, and T.J. Greytak, *Phys. Rev. Lett.* **81**, 3811 (1998).
- [5] C.C. Bradley, C.A. Sackett, J.J. Tollett, and R.G. Hulet, *Phys. Rev. Lett.* **75**, 1687 (1995); C.C. Bradley, C.A. Sackett, and R.G. Hulet, *ibid.* **78**, 985 (1997); C.C. Bradley, C.A. Sackett, J.J. Tollett, and R.G. Hulet, *ibid.* **79**, 1170 (1997).
- [6] M. Edwards and K. Burnett, *Phys. Rev. A* **51**, 1382 (1995); P.A. Ruprecht, M.J. Holland, K. Burnett, and M. Edwards, *ibid.* **51**, 4704 (1995).
- [7] G. Baym and C.J. Pethick, *Phys. Rev. Lett.* **76**, 6 (1996).
- [8] J.L. Roberts, N.R. Claussen, S.L. Cornish, E.A. Donley, E.A. Cornell, and C.E. Wieman, *Phys. Rev. Lett.* **86**, 4211 (2001); E.A. Donley, N.R. Claussen, S.L. Cornish, J.L. Roberts, E.A. Cornell, and C.E. Wieman, *Nature (London)* **412**, 295 (2001); N.R. Claussen, E.A. Donley, S.T. Thompspon, and C.E. Wieman, *Phys. Rev. Lett.* **89**, 010401 (2002).
- [9] W.C. Stwalley, *Phys. Rev. Lett.* **37**, 1628 (1976); E. Tiesinga, A.J. Moerdijk, B.J. Verhaar, and H.T.C. Stoof, *Phys. Rev. A* **46**, R1167 (1992).
- [10] S. Inouye, M.R. Andrews, J. Stenger, H.-J. Miesner, D.M. Stamper-Kurn, and W. Ketterle, *Nature (London)* **392**, 151 (1998); P. Courteille, R.S. Freeland, D.J. Heinzen, F.A. van Abeelen, and B.J. Verhaar, *Phys. Rev. Lett.* **81**, 69 (1998).
- [11] A. Gammal, T. Frederico, and L. Tomio, *Phys. Rev. A* **64**, 055602 (2001).
- [12] A. Gammal, T. Frederico, L. Tomio, and Ph. Chomaz, *J. Phys. B* **33**, 4053 (2000).
- [13] F. Dalfovo, S. Giorgini, L.P. Pitaevskii, and S. Stringari, *Rev. Mod. Phys.* **71**, 463 (1999).
- [14] Y. Kagan, A.E. Muryshev, and G.V. Shlyapnikov, *Phys. Rev. Lett.* **81**, 933 (1998).
- [15] M. Edwards and K. Burnett, *Phys. Rev. A* **51**, 1382 (1995); P.A. Ruprecht, M.J. Holland, K. Burnett, and M. Edwards, *ibid.* **51**, 4704 (1995).
- [16] E. Timmermans, P. Tommasini, M. Hussein, and A. Kerman, *Phys. Rep.* **315**, 199 (1999).
- [17] H. Saito and M. Ueda, *Phys. Rev. Lett.* **86**, 1406 (2001); *Phys. Rev. A* **63**, 043601 (2001); **65**, 033624 (2002).
- [18] V.S. Filho, A. Gammal, T. Frederico, and L. Tomio, *Phys. Rev. A* **62**, 033605 (2000).
- [19] J.M. Gerton, C.A. Sackett, B.J. Frew, and R.G. Hulet, *Phys. Rev. A* **59**, 1514 (1999).
- [20] R.J. Deissler and K. Kaneko, *Phys. Lett. A* **119**, 397 (1987); R.J. Deissler, *J. Stat. Phys.* **54**, 1459 (1989).
- [21] S.H. Strogatz, *Nonlinear Dynamics and Chaos* (Addison-Wesley Publishing Company, Reading, MA, 1994).
- [22] V.S. Filho, F.K. Abdullaev, A. Gammal, and L. Tomio, *Phys. Rev. A* **63**, 053603 (2001).
- [23] A. Eleftheriou and K. Huang, *Phys. Rev. A* **61**, 043601 (2000).